

# Cosmological constraints combining $H(z)$ , CMB shift and SNIa observational data

Ruth Lazkoz<sup>1</sup> and Elisabetta Majerotto<sup>2</sup>

<sup>1</sup>*Fisika Teorikoa, Euskal Herriko Unibertsitatea, 48080 Bilbao, Spain*

<sup>2</sup>*Institute of Cosmology & Gravitation, University of Portsmouth, Portsmouth PO1 2EG, UK*

*E-mail: ruth.lazkoz@ehu.es and elisabetta.majerotto@port.ac.uk*

(Dated: November 3, 2018)

Recently  $H(z)$  data obtained from differential ages of galaxies have been proposed as a new geometrical probe of dark energy. In this paper we use those data, combined with other background tests (CMB shift and SNIa data), to constrain a set of general relativistic dark energy models together with some other models motivated by extra dimensions. Our analysis rests mostly on Bayesian statistics, and we conclude that  $\Lambda$ CDM is at least substantially favoured, and that extradimensional models are less favoured than general relativistic ones.

## I. INTRODUCTION

The almost undisrupted flow of data potentially useful for cosmological model selection and parameter fitting provides day by day a clearer picture of the evolution of the Universe, which according to a wide consensus seems to be currently accelerating. Yet it is uncertain how strong the conclusions of these sorts of investigation are, as there are not only statistical uncertainties to worry about, but possible theoretical biasing in the tests used.

This being the situation, the community is eager to be able to devise new tests and/or improve the understanding of the shortcomings of the existing ones towards refining them. The underlying hope is that, at least from a phenomenological perspective, cosmologists will eventually be able to tell with high precision how fast the Universe is expanding at present, how long this speed up has lasted, and how the acceleration rate has changed over the recent past.

Recently Simon et al. [1] have published Hubble function  $H(z)$  data extracted from differential ages of passively evolving galaxies. The use of these data to constrain the background evolution of the Universe is interesting for several reasons. First, it can be used together with other cosmological tests in order to get useful consistency checks or tighter constraints on models. Second, in contrast to standard candle luminosity distances or standard ruler angular diameter distances, the Hubble function is not integrated over. This will allow, mostly in the future, when the systematic errors associated with the cluster physics have been reduced, to get cleaner constraints on the cosmological parameters. The same data have also been recently used in [2, 3] to constrain several cosmological models. In this paper we use them in combination with the latest SNe Ia set compiled by Davis et al. [4] and the CMB shift parameter as calculated by Wang and Mukherjee [5] from WMAP 3 [6]. In contrast to other works, we have chosen not to use the baryon acoustic oscillations (BAO) data because, as pointed out in [7], there is a level of uncertainty in the use of the measure  $A$  given in [8] to test non- $\Lambda$ CDM models.

We have chosen to put constraints on 6 different cos-

mological models that show late-time acceleration (see e.g. [9, 10, 11]). For all of them we have assumed flat space, consistent with the inflationary prediction that the curvature density parameter  $\Omega_k \sim 0$  [12] and with the results obtained by CMB experiments [6, 13].

Three of the models are dark energy models while in the remaining three models the acceleration arises from or is modified by a five-dimensional modification of gravity motivated by extra dimensional physics. One also can group these models by pairs according to the number of parameters apart from  $H_0$ .  $\Lambda$ CDM and DGP [14, 15] have only one parameter, i.e. the matter density parameter. QCDM, i.e. dark energy parametrized as a perfect fluid with a constant equation of state, and LDGP, a non self-accelerating solution for the DGP action [16], add to the matter density one further parameter: the equation of state and the crossover scale (i.e. the scale at which the 5-dimensional behaviour becomes effective), respectively. The last two models chosen are the Chevalier-Polarski-Linder parametrization [17, 18] (which contains two parameters characterizing the evolution of the equation of state) and the QDGP model [19], a phenomenological extension of the LDGP model, where the cosmological constant is replaced by a dark energy fluid with a constant equation of state. Similar analyses of a subset of these models using recent datasets partially overlapping with ours have been done in [20, 21, 22] and our work may be complementary to that.

The plan of the paper is as follows. In Sec. II we outline the models to be investigated and the corresponding forms of  $H(z)$ . Then, in Sec. III we give details of the three datasets considered, and we explain how they can be used to constrain the background of cosmological models. After that, in Sec. IV we review the concepts and techniques we resort to in our statistical analysis of the data. Finally, we present our results and conclusions in Sec. V (accompanied by some additional statistical information and considerations about the effective equations of state in the different models in the Appendices).

## II. MODELS AND PARAMETRIZATIONS

As discussed in detail in [23], extracting information about the properties of dark energy from a reconstruction of  $H(z)$  is not in principle problematic from the mathematical perspective, but it is hard in practice because one only has at hand a discrete set of noisy data (for several redshifts) from which one wishes to infer information valid for all redshift values within a given interval. The various approaches to confronting models with data are based on deriving the luminosity distance  $D_L(z)$  [24],  $w_{de}(z)$  [17, 18, 25, 26] or  $H(z)$  [15, 16, 19, 27, 28].

Here we will use the second approach and compare to observations six cosmological models altogether: the models can be grouped in pairs according to the number of parameters (one, two or three); in addition each pair will contain one general relativistic dark energy model and one model inspired by extradimensional modifications to gravity.

### A. LCDM

In general, if we consider a general relativistic model of dark energy with an equation of state that depends on the redshift,  $w_{de}(z)$ , the expression for  $H^2(z)$  obeys

$$\frac{H^2(z)}{H_0^2} = \Omega_m(1+z)^3 + (1-\Omega_m) \exp \left[ 3 \int_0^z \frac{1+w_{de}(x)}{1+x} dx \right], \quad (1)$$

where one assumes that in addition to dark energy the Universe contains dust (dark matter and baryons).

The LCDM model corresponds to the choice  $w_{de}(z) = -1$ , i.e. dark energy is a cosmological constant  $\Lambda$ . Thus

$$\frac{H^2(z)}{H_0^2} = \Omega_m(1+z)^3 + 1 - \Omega_m, \quad (2)$$

and the free parameter of the model is  $\Omega_m$ . LCDM is consistent with all data, but there is a theoretical problem in explaining the observed value of  $\Lambda$ .

### B. DGP

The dark gravity model inspired by the Dvali-Gabadadze-Porrati (DGP) braneworld model [14] was given by Deffayet [15], and it represents a simple alternative to the standard LCDM cosmology, with the same number of parameters.

In this model the late Universe self-accelerates, not because of dark energy, which is absent, but rather due to an infrared modification of gravity. Explicitly one has

$$\frac{H(z)}{H_0} = \frac{1-\Omega_m}{2} + \sqrt{\frac{(1-\Omega_m)^2}{4} + \Omega_m(1+z)^3}. \quad (3)$$

One can define an effective dark energy equation of state  $w_{\text{eff}}$  by imposing  $H^2 = H_0^2 \Omega_m(1+z)^3 + 8\pi G \rho_{\text{eff}}/3$  along with  $\dot{\rho}_{\text{eff}} + 3H(1+w_{\text{eff}})\rho_{\text{eff}} = 0$  to obtain, implicitly

$$w_{\text{eff}} = \frac{\frac{2}{3}(1+z) \frac{d \ln E(z)}{dz} - 1}{1 - E^{-2}(z) \Omega_m(1+z)^3}, \quad (4)$$

where  $E(z) \equiv H(z)/H_0$ , and explicitly

$$w_{\text{eff}}(z) = \frac{\Omega_m - 1 - \sqrt{(1-\Omega_m)^2 + 4\Omega_m(1+z)^3}}{2\sqrt{(1-\Omega_m)^2 + 4\Omega_m(1+z)^3}}. \quad (5)$$

For this scenario one can see that  $\lim_{z \rightarrow -1} w_{\text{eff}} = -1$ , so the final asymptotic state is a de Sitter model.

### C. QCDM

This model arises from the simplest generalization of LCDM, which consists in taking a constant value of  $w_{de} = w$  different, in general, from  $-1$ , so one gets

$$\frac{H^2(z)}{H_0^2} = \Omega_m(1+z)^3 + (1-\Omega_m)(1+z)^{3(1+w)}. \quad (6)$$

Despite its simplicity, this model can prove useful, as a preference for this parametrization over the LCDM case will provide support for the evolutionary nature of dark energy.

### D. LDGP

This model represents the non self-accelerating branch of DGP (the two separate branches of DGP arise from the two possible ways to embed the 4D brane universe in the 5D spacetime; see also [16, 29] for further explanation). To generate acceleration a cosmological constant is needed. There are two main features of this model. One is the screening effect on  $\Lambda$  due to the presence of the extra dimension, that allows for a higher value of the cosmological constant. The other is the possibility of having effective phantom behaviour without any phantom field and any of the associated instabilities. In addition, this model does not have ghosts, unlike the self-accelerating DGP.

The evolution of the model is governed by the relation

$$\frac{H(z)}{H_0} = \sqrt{\Omega_m(1+z)^3 + \Omega_\Lambda} - \sqrt{\Omega_{r_c}}, \quad (7)$$

where on the one hand  $\Omega_\Lambda = 1 + 2\sqrt{\Omega_{r_c}} - \Omega_m$  for the requirement of flatness (see [29]), and on the other hand the parameter  $\Omega_{r_c}$  is related to the crossover scale which signals the transition from the general relativistic to the modified gravity regime (see again [16] for details). Observational constraints on this particular model using SN, CMB shift and BAO data were studied in [29], where it

was found that statistically the best fit corresponded to the LCDM limit of the model.

The same procedure to obtain  $w_{\text{eff}}$  that we mentioned in the DGP model applies here, so one will have, from Eq. (4),

$$w_{\text{eff}}(z) = -1 - \frac{\sqrt{\Omega_{r_c}}\Omega_m(1+z)^3}{[\Omega_\Lambda - 2\sqrt{\Omega_{r_c}}E(z)][\sqrt{\Omega_{r_c}} + E(z)]}. \quad (8)$$

### E. Chevallier-Polarski-Linder Ansatz

This is a widely used Ansatz, which generalizes QCDM to allow for evolution in the dark energy equation of state, as required by most realistic scalar field models. (It was first discussed in [17], and reintroduced independently in [18].)

Explicitly it corresponds to  $w_{\text{de}}(z) = w_0 + w_1(1 - (1+z)^{-1})$  and therefore

$$\frac{H^2(z)}{H_0^2} = \Omega_m(1+z)^3 + (1 - \Omega_m)(1+z)^{3(1+w_0+w_1)}e^{-3\frac{w_1z}{1+z}}. \quad (9)$$

Among its desirable features two stand out: first, this parametrization of dark energy remains finite at large redshifts, and second, the physical interpretation of the model is simple as the parameter  $w_1$  is a measure of the scalar field potential slow roll factor  $V'/V$  in the case of quintessence [18].

### F. QDGP

This model, introduced in [19], is a generalization of LDGP where the cosmological constant is replaced by dark energy with a constant equation of state  $w$ , in general different from  $-1$ , that represents a new parameter of the model. The modified 4D Friedman equation has the following form:

$$\frac{H(z)}{H_0} = \sqrt{\Omega_m(1+z)^3 + \Omega_w(z) + \Omega_{r_c}} - \sqrt{\Omega_{r_c}} \quad (10)$$

where  $\Omega_w(z) \equiv (1 + 2\sqrt{\Omega_{r_c}} - \Omega_m)(1+z)^{3(1+w)}$ . Clearly, in this case too one can make use of Eq. (4) to derive  $w_{\text{eff}}$ :

$$w_{\text{eff}} = -1 + \frac{(1+w)\Omega_w(z)E(z) - \sqrt{\Omega_{r_c}}\Omega_m(1+z)^3}{[E(z) + \sqrt{\Omega_{r_c}}][\Omega_w(z) - 2E(z)\sqrt{\Omega_{r_c}}]}. \quad (11)$$

## III. OBSERVATIONAL TESTS

### A. Hubble parameter observations

The Hubble parameter depends on the differential age of the Universe in terms of redshift, specifically

$$H(z) = -\frac{1}{1+z} \frac{dz}{dt}. \quad (12)$$

Thus, measuring  $dt/dz$  allows us to determine  $H(z)$ . As described first in [30] and in [1, 31], it is possible to use absolute ages of passively evolving galaxies to compute values of  $dt/dz$ . The galaxy spectral data used by [1] come from the Gemini Deep Deep Survey [32] and archival data [33]. In broad terms, the authors of these references bin together galaxies with a redshift separation which is small enough so that the galaxies in the bin have roughly the same age; then, they calculate age differences between bins which have a small age difference which is at the same time larger than the error in the age itself [1]. The outcome of this process is a set of 9 values of the Hubble parameter versus redshift (see Table I). A particularly nice feature of this test is that differential ages are less sensitive to systematic errors than absolute ages [34].

TABLE I:  $H(z)$  data from [1] (in units of  $\text{km s}^{-1}\text{Mpc}^{-1}$ )

$z$	$H(z)$	$\sigma$
0.09	69	12
0.17	83	8.3
0.27	70	14
0.4	87	17.4
0.88	117	23.4
1.3	168	13.4
1.43	177	14.2
1.53	140	14
1.75	202	40.4

Observed values of  $H(z)$  can be used to place constraints on different models of the expansion history of the Universe by minimizing the quantity

$$\chi_{\text{H}}^2(H_0, \{\theta_i\}) = \sum_{j=1}^9 \frac{(H(z_j; \{\theta_i\}) - H_{\text{obs}}(z_j))^2}{\sigma_{\text{H},j}^2}. \quad (13)$$

This test has already been used to constrain several cosmological models in [2, 3], and it does not seem to provide tight constraints on its own, so it seems necessary to combine it with other tests. Now, since one of the other tests we are using (the CMB shift) does not constrain  $H_0$  we will regard this parameter as a nuisance one, and so it will be more convenient to marginalize over it (see for instance [35]) and work with the quantity

$$\hat{\chi}_{\text{H}}^2(\{\theta_i\}) = -2 \log \left( \int \pi_{\text{H}}(H_0) e^{-\chi_{\text{H}}^2(H_0, \{\theta_i\})} dH_0 \right). \quad (14)$$

The quantity  $\pi_H(H_0)$  is a so called prior probability function (see section IV) which reflects some previous knowledge about preferred values of  $H_0$ . We have independent evidence from the Chandra X-ray observatory giving  $H_0 = 77 \pm 4 \text{ kms}^{-1}\text{Mpc}^{-1}$  [36]. This result is consistent with the 3 year WMAP dataset result  $H_0 = 73 \pm 3 \text{ kms}^{-1}\text{Mpc}^{-1}$  [6] and with the Hubble Space Telescope key project result  $H_0 = 73 \pm 8 \text{ kms}^{-1}\text{Mpc}^{-1}$  [37]. Here we choose to use the Chandra X-ray result (for statistical independence with respect to the other tests to be used later) and use this result to place a Gaussian prior on  $H_0$  so that

$$\pi_H(H_0) = \frac{1}{\sqrt{2\pi}\sigma_{H_0}} e^{-(H_0 - H_0^{obs})^2 / 2\sigma_{H_0}^2} \quad (15)$$

where obviously  $H_0^{obs} = 77$  and  $\sigma_{H_0} = 4$ .

### B. The Davis et al. 2007 dataset

This dataset is one of the latest supernovae catalogs to be completed. It consists of 192 SNe classified as type Ia up to a redshift of  $z = 1.755$  [4]. The authors combine the set compiled by [38] and the 30 new SNe data at high redshift ( $0.216 \leq z \leq 1.755$ ) recently discovered with the Hubble Space Telescope (HST) [11]. The first of those two sets consists of the addition of three smaller datasets. The first subset is made of the SNe Ia data from the ESSENCE project [38], a ground-based survey designed to detect about 200 SNe Ia in the range  $z = 0.2-0.8$ . The second is made of the Supernova Legacy Survey (SNLS) [39] data. These have been refitted by [38] with the same lightcurve fitter used for the ESSENCE data. The third subset corresponds to the nearby SNe already presented in [9, 40, 41] as refitted and used by [38]. As regards the HST SNe, it has been necessary to perform a normalization since the refitting of the HST lightcurves with the fitter used for the ESSENCE data is still in progress. The normalization has been done using the low redshift sample common to both sets and the error in the normalization is included in the distance errors for the HST SNe. Summarizing, the Davis et al. dataset consists of 60 ESSENCE supernovae, 57 SNLS supernovae, 45 nearby supernovae and 30 HST supernovae. It is available at <http://www.dark-cosmology.dk/archive/SN>, <http://braeburn.pha.jhu.edu/~ariess/R06> and <http://www.ctio.noao.edu/essence>.

The statistical best fits of theoretical forms of  $H(z)$  using supernovae data rest on the definition for the distance modulus

$$\mu_{\text{th}}(z_i) = 5 \log_{10}(d_L(z; \{\theta_i\})) + \mu_0 \quad (16)$$

where

$$d_L(z; \{\theta_i\}) = (1+z) \int_0^z \frac{H_0 dz}{H(z; H_0, \{\theta_i\})} \quad (17)$$

is the dimensionless luminosity distance which is related to its dimensional counterpart through  $D_L(z; H_0, \{\theta_i\}) = c d_L(z; \{\theta_i\}) / H_0$ .

The best fits are obtained by minimizing the quantity (see Sec. IV)

$$\chi_{\text{SN}}^2(\mu_0, \{\theta_i\}) = \sum_{j=1}^{192} \frac{(\mu_{\text{th}}(z_j; \mu_0, \{\theta_i\}) - \mu_{\text{obs}}(z_j))^2}{\sigma_{\mu,j}^2}, \quad (18)$$

where the  $\sigma_{\mu,j}$  are the measurement variances [4]. The nuisance parameter  $\mu_0$  encodes the Hubble parameter and the absolute magnitude  $M$  [42] and has to be marginalized over [35]. So one will actually be working with the quantity

$$\tilde{\chi}_{\text{SN}}^2(\{\theta_i\}) = -2 \log \left( \int e^{-\chi_{\text{SN}}^2(\mu_0, \theta_1, \dots, \theta_n)} d\mu_0 \right). \quad (19)$$

A frequently used alternative [43], consists in minimizing the quantity

$$\tilde{\chi}_{\text{SN}}^2(\{\theta_i\}) = c_1 - \frac{c_2^2}{c_3} \quad (20)$$

with respect to the other parameters. Here

$$c_1 = \sum_{j=1}^{192} \frac{(\mu_{\text{th}}(z_j, \mu_0 = 0, \{\theta_i\}) - \mu_{\text{obs}}(z_j))^2}{\sigma_{\mu,j}^2} \quad (21)$$

$$c_2 = \sum_{j=1}^{192} \frac{\mu_{\text{th}}(z_j, \mu_0 = 0, \{\theta_i\}) - \mu_{\text{obs}}(z_j)}{\sigma_{\mu,j}^2} \quad (22)$$

$$c_3 = \sum_{j=1}^{192} \frac{1}{\sigma_{\mu,j}^2}. \quad (23)$$

It is trivial to see  $\tilde{\chi}_{\text{SN}}^2$  is just a version of  $\chi_{\text{SN}}^2$  minimized with respect to  $\mu_0$ . To that end it suffices to notice that [43]

$$\chi_{\text{SN}}^2(\mu_0, \{\theta_i\}) = c_1 - 2c_2\mu_0 + c_3\mu_0^2, \quad (24)$$

which clearly becomes minimum for  $\mu_0 = c_2/c_3$ , and so we can see  $\tilde{\chi}_{\text{SN}}^2(\{\theta_i\}) \equiv \chi_{\text{SN}}^2(\mu_0 = 0, \{\theta_i\})$ . Furthermore, one can check that the difference between  $\tilde{\chi}_{\text{SN}}^2$  and  $\tilde{\chi}_{\text{SN}}^2$  is negligible and therefore we will just use the first of them.

### C. The CMB shift

The CMB shift  $R$  is arguably the parameter with least model-dependence among those which can be inferred from CMB data, provided that the dark energy density parameter is negligible at recombination, and it does not depend on  $H_0$ . It is directly proportional to the ratio of the locations of the first peak in the temperature angular power spectrum in the model one wants to characterize ( $l_1^{TT}$ ) and in a reference flat  $\Lambda$ CDM model ( $l_1'^{TT}$ ), that is,

$$R \equiv 2 \frac{l_1^{TT}}{l_1'^{TT}} \approx H_0 \sqrt{\Omega_m} \int_0^{z_{\text{rec}}} \frac{dz}{H(z)}, \quad (25)$$

where  $z_{\text{rec}}$  is the redshift of recombination (a factor of 2 has deliberately been introduced so as to reconcile the different definitions of the shift parameter in the literature). The approximate expression in the last equality of (25) is the definition given in [44] and when we turn to numerical tests we will take it as exact, i.e. we will ignore the fact that it is only approximately equal to other definitions. In the following lines we will show how to obtain this approximate expression for  $R$ . In an arbitrary model one has

$$l_1^{TT} = \pi \frac{D_A(z_{\text{rec}})}{r_s(z_{\text{rec}})} \quad (26)$$

where the last scattering sound horizon scale  $r_s(z_{\text{rec}})$  is given by

$$r_s(z_{\text{rec}}) = a_{\text{rec}} \int_0^{a_{\text{rec}}} \frac{c_s(a) da}{a^2 H(a)}, \quad (27)$$

with  $c_s$  the sound speed in the model, and (under the assumption of flatness) the sound horizon angular diameter distance is in turn given by

$$D_A(z_{\text{rec}}) = \frac{c}{1 + z_{\text{rec}}} \int_0^{z_{\text{rec}}} \frac{dz}{H(z)}. \quad (28)$$

Arguably, one can take  $c_s(a)$  to be constant, and in addition we will take  $a_{\text{rec}}$  and  $a_{\text{eq}}$  to be model independent. Approximate expressions will be obtained using  $1 \gg a_{\text{rec}} \gg a_{\text{eq}}$ . For a fiducial matter-radiation model one gets <sup>1</sup>

$$r'_s(z_{\text{rec}}) = \frac{a_{\text{rec}}}{H_0 \sqrt{\Omega'_m}} \int_0^{a_{\text{rec}}} \frac{c_s da}{(a + a_{\text{eq}})^{1/2}} = \frac{2c_s}{H_0 \sqrt{\Omega'_m}} (\sqrt{a_{\text{eq}} + a_{\text{rec}}} - \sqrt{a_{\text{eq}}}), \quad (29)$$

but if one makes the more stringent assumption that the fiducial model is a  $\Lambda$ CDM one ( $\Omega'_m = 1$ ) then from the latter it follows that

$$r'_s(z_{\text{rec}}) \approx \frac{c_s}{H_0} a_{\text{rec}}^{3/2}, \quad (30)$$

and

$$D'_A \approx \frac{2c}{H_0} a_{\text{rec}}. \quad (31)$$

On the other hand, and in an arbitrary model

$$r_s(z_{\text{rec}}) \approx \frac{c_s}{H_0 \sqrt{\Omega'_m}} a_{\text{rec}}^{3/2}, \quad (32)$$

so using the definition in Eq. (26) combined with Eqs. (28,30,31,32), one obtains Eq. (25). Constraints on the parametrizations of  $H(z)$  using reported values of the

CMB shift (based on observations) will be obtained from minimization of the quantity (see Sec. IV)

$$\chi_{\text{CMB}}^2(\{\theta_i\}) = \frac{(R(z_{\text{rec}}; \{\theta_i\}) - R_{\text{obs}}(z_{\text{rec}}))^2}{\sigma_R^2}. \quad (33)$$

We use the value  $R = 1.70 \pm 0.03$  of the CMB shift parameter calculated by [5] from the WMAP 3 data [6] (for the computed value  $z_{\text{rec}} = 1090$ ). Recently some points regarding the use of the CMB shift parameter have been raised and discussed by [47, 48, 49] and this is an issue that deserves additional clarification. Furthermore, one must be cautious, when weighting the conclusions reached using the CMB shift as it extends the redshift integration out to very large redshift, so that arbitrary parametrizations called to be applicable for such large redshift range can be very sensitive to errors.

#### IV. STATISTICS AND DATA ANALYSIS

Parameter estimation in the context of a given (cosmological) model depending on some parameters has two ultimate goals: one is the determination of the “most likely” values of the parameters to yield a series of available observational data, the other is measuring our degree of confidence in the fact that those data were generated by values of those parameters lying in an estimated interval. A related task is to compare different models using information retrieved in the parameter estimation process. The estimators used in both these jobs (parameter estimation and model comparison) are different in the two main approaches to statistics (frequentist and Bayesian). In the remainder of this section we give a short account of these topics.

##### A. Parameter estimation

By definition  $\mathcal{L}(\{d_j\}|\{\theta_i\}, \mathcal{M})$  represents the the unnormalized probability density function (aka likelihood) that one measures the data  $\{d_j\}$  given the model  $\mathcal{M}$  is true and its parameters take values  $\{\theta_i\}$  [50]. Even though we will try to keep the discussion in this section as general as possible, when we turn to analyze particular datasets we will assume as customary that the measurements are normally distributed around their true value so that

$$\mathcal{L}(\{d_j\}|\{\theta_i\}, \mathcal{M}) \propto e^{-\chi^2(\{\theta_i\})/2}. \quad (34)$$

The probability density function  $p(\{\theta_i\}|\{d_j\}, \mathcal{M})$  of the parameters to have values  $\{\theta_i\}$  under the assumption that the true model is  $\mathcal{M}$  and provided that the available observational data are  $\{d_j\}$  reads [50]

<sup>1</sup> We present our expression in a fashion more similar to that in Eq. (10) of Ref [45] although it is completely equivalent to Eq.

(18) in Ref. [46]

$$p(\{\theta_i\}|\{d_j\}, \mathcal{M}) = \frac{\mathcal{L}(\{d_j\}|\{\theta_i\}, \mathcal{M})\pi(\{\theta_i\}, \mathcal{M})}{\int \mathcal{L}(\{d_j\}|\{\theta_i\}, \mathcal{M})\pi(\{\theta_i\}, \mathcal{M})d\theta_1 \dots d\theta_n}. \quad (35)$$

In the Bayesian framework  $p(\{\theta_i\}|\{d_j\}, \mathcal{M})$  and  $\pi(\{\theta_i\}, \mathcal{M})$  are respectively called the posterior and prior probability density functions (pdf) [50, 51, 52, 54, 57]. The prior pdf encodes all previous knowledge about the parameters before the observational data have been collected. It may be regarded as subjective up to a certain point, but its use is compulsory in the Bayesian approach, which is arguably the approach to be used for theoretical frameworks which do not admit repetition of experiments (we only have one universe to enquire about).

Parameter estimation in the Bayesian framework is based on maximizing the posterior pdf  $p(\{\theta_i\}|\{d_j\}, \mathcal{M})$ , whereas in a “strict” frequentist approach one just maximizes  $\mathcal{L}(\{d_j\}|\{\theta_i\}, \mathcal{M})$ . When one uses flat priors in the Bayesian approach then the same conclusions are drawn from both approaches and then the difference turns to be conceptual only [51, 52, 53]. Interestingly, this kind of prior, which is also called the top-hat prior, is the most popular one in usual practise, but this does not necessarily mean it gives a fair representation of the state of knowledge before the experiment is carried out, and this usually requires physical insight into the problem (sometimes priors rest upon symmetry considerations) [53]<sup>2</sup>.

The second step toward constraining parameters satisfactorily is to construct credible intervals [54, 55]. We will for a while simplify our notation and let

$$p(\{\theta_i\}|\{d_j\}, \mathcal{M}) \equiv p(\theta_1, \dots, \theta_n). \quad (36)$$

In the Bayesian approach [54] the 68% credible intervals on the parameter  $\theta_i$  will be given as  $\theta_i = x_{-y}^{+z}$  with  $x, y, z$  calculated as follows. Here  $x$  will be the median of the marginal probability density function

$$p(\theta_i) = \int p(\theta_1, \dots, \theta_n)d\theta_1 \dots d\theta_{i-1}d\theta_{i+1} \dots d\theta_n. \quad (37)$$

The median  $x$  is calculated from

$$\int_{\theta_{ii}}^x p(\theta_i)d\theta_i = 0.5 \times \int p(\theta_i)d\theta_i. \quad (38)$$

Similarly,  $y$  is calculated from

$$\int_{\theta_{ii}}^{x-y} p(\theta_i)d\theta_i = ((1 - 0.68)/2) \times \int p(\theta_i)d\theta_i, \quad (39)$$

<sup>2</sup> Some people work in a “mixed” approach and consider priors but then follow frequentist procedures.

and  $z$  is calculated from

$$\int_{x+z}^{\theta_{iu}} p(\theta_i)d\theta_i = ((1 - 0.68)/2) \times \int p(\theta_i)d\theta_i. \quad (40)$$

For marginalized normalized likelihood functions (i.e. posteriors) and likelihood contours see Figs. 1-10. The parameters  $\theta_{il}$  and  $\theta_{iu}$  entering the definitions of  $y$  and  $z$  are respectively a lower and an upper bound which should either be given by some physical restriction, or alternatively be chosen so that the conditions  $p(\theta_{il}) \approx 0$  and  $p(\theta_{iu}) \approx 0$  are satisfied to the desired degree of accuracy. Hence, the probability to get the observed values of the different physical quantities into play is 0.68 if  $\theta_i$  lies in the range  $[x - y, x + z]$ . The modification required so as to calculate the 95% credible interval is straightforward.

In cases with strongly asymmetric posteriors, one will have to resort to alternative ways to report credible intervals [56]. This will be the case in two of the models under study in this paper, and details will be given below.

In order to calculate the confidence intervals (correspondent of the credible intervals of Bayesian statistics) in the frequentist approach one has to calculate the mode of  $\mathcal{L}(\theta_i)$ , which is the value of  $\theta_i$  which maximizes  $\mathcal{L}(\theta_i)$ . We will denote this value as  $\theta_{imd}$ . The boundaries of the 68% confidence interval are calculated by finding the two values of  $\theta_i$  for which  $\mathcal{L}(\theta_i) = \mathcal{L}(\theta_{imd})e^{-1/2}$  [55], whereas the 95% confidence interval is obtained by the same recipe, except that the exponent  $-1/2$  must be replaced by  $-2$ . We will not use this way of calculating confidence intervals because it is exact only in gaussian situations (see Eq. (34)), but we will rather do it the Bayesian way.

In two of our models (specifically LDGP and QDGP) it happens that, due to nonphysicality reasons, the allowed region of one of the parameters ( $\Omega_{r_c}$ ) is truncated by a theoretical cut. This sharp restriction demands a modification of the definition of credible intervals. Let us denote this parameter as  $\theta_*$  for simplicity (and consistency with the notation in this section). The truncation is such that  $\theta_{*l} = \theta_{*md}$ , so the 68% credible interval on  $\theta_*$  will be reported as  $\theta_* = x^{+z}$ , where  $x$  will now denote  $\theta_{*md}$  and  $z$  will be calculated as

$$\int_x^z p(\theta_*)d\theta_* = 0.68 \times \int p(\theta_*)d\theta_*. \quad (41)$$

Table II summarizes results.

## B. Model comparison

A popular but not too refined way to rate goodness of models in the frequentist approach is to compare values of the quantity  $-2 \log \max\{\mathcal{L}(\theta_1, \dots, \theta_n)\}/\text{dof} \equiv \max\{\chi^2(\theta_1, \dots, \theta_n)\}$  where dof stands for the number of degrees of freedom of the model, which in turn is the number of observational data point minus the number of parameters. Nevertheless, in general  $\max\{\mathcal{L}(\theta_1, \dots, \theta_n)\} \neq \mathcal{L}(\theta_{1\text{md}}, \dots, \theta_{n\text{md}})$ ; if we let  $\max\{\mathcal{L}(\theta_1, \dots, \theta_n)\} = \mathcal{L}(\theta_{1\text{bf}}, \dots, \theta_{n\text{bf}})$  then the vector  $(\theta_{1\text{bf}}, \dots, \theta_{n\text{bf}})$  will represent what is usually referred to as the best fit.

In the Bayes approach, the preferred estimator is the evidence [57]. It does not rely exclusively on the best-fitting parameters of the model, in contrast, it informs about how well the parameters of the model fit the data, after doing an averaging over all the parameter values that were theoretically plausible before the measurement ever took place [58].

We denote Bayes evidence as  $\mathcal{E}(\mathcal{M}) = p(\{d_j\}|\mathcal{M})$ , and it is defined as the probability of the data  $\{d_j\}$  given the model  $\mathcal{M}$ , that is,

$$\mathcal{E}(\mathcal{M}) = \int \pi(\{\theta_i\}, \mathcal{M}) \mathcal{L}(\{d_j\}|\{\theta_i\}, \mathcal{M}) d\theta_1 \dots d\theta_n \quad (42)$$

where  $\pi(\{\theta_i\}, \mathcal{M})$  is the model's prior on the set of parameters, normalized to unity (i.e.  $\int \pi(\{\theta_i\}, \mathcal{M}) d\theta_1 \dots d\theta_n = 1$ ). The most common choice is the top hat prior, so that one rewrites Bayes evidence as

$$\mathcal{E}(\mathcal{M}) = \frac{\int_{\theta_{1\text{min}}}^{\theta_{1\text{max}}} \dots \int_{\theta_{n\text{min}}}^{\theta_{n\text{max}}} \mathcal{L}(\theta_1, \dots, \theta_n) d\theta_1 \dots d\theta_n}{\int_{\theta_{1\text{min}}}^{\theta_{1\text{max}}} \dots \int_{\theta_{n\text{min}}}^{\theta_{n\text{max}}} d\theta_1 \dots d\theta_n}. \quad (43)$$

Now, to realize of the usefulness of the Bayes evidence towards our final goal, which is model selection, note that in Bayesian statistics the preference of model  $\mathcal{M}_i$  over model  $\mathcal{M}_j$  given the data  $\{d_k\}$  is estimated through the quotient

$$\frac{p(\mathcal{M}_i|\{d_k\})}{p(\mathcal{M}_j|\{d_k\})} = \frac{\mathcal{E}_i(\mathcal{M}_i) \pi_i(\mathcal{M}_i)}{\mathcal{E}_j(\mathcal{M}_j) \pi_j(\mathcal{M}_j)}. \quad (44)$$

On the other hand, the Bayes factor  $B_{ij}$  for any two models  $\mathcal{M}_i$  and  $\mathcal{M}_j$  is defined as

$$B_{ij} = \frac{\mathcal{E}_i(\mathcal{M}_i)}{\mathcal{E}_j(\mathcal{M}_j)} \quad (45)$$

so if, as in usual practise, one assumes no prior preference of one model over the other, that is,  $\pi_i(\mathcal{M}_i) = \pi_j(\mathcal{M}_j) = 1/2$ , one finally has

$$\frac{p(\mathcal{M}_i|\{d_k\})}{p(\mathcal{M}_j|\{d_k\})} = B_{ij}. \quad (46)$$

We report values of the evidences and Bayes factor for the models considered here in Table IV (see Table III for priors). Values of the Bayes factor could be used to attribute evidence to the model  $\mathcal{M}_i$  against the model  $\mathcal{M}_j$  using Jeffreys' scale [59] which regards evidences of one model against the other as not significant, substantial, strong or decisive depending on values of  $\ln(B_{ij})$ . Recently a the refinement of this scale has been proposed by Wasserman [60]. These scales are of course subjective and one can question how illustrating they actually are, but the underlying philosophy is that the Bayes factor is a ratio of odds in the case there is no preference of one model over the other, so for the benefit of the readers which prefer a more objective report of our results we give, in Table V, the ratio of odds of different pairs of models among those under consideration, which we will express as  $\mathcal{O}_{ij} \equiv B_{ij} : 1$  in the cases where  $B_{ij} \geq 1$ , whereas for the sake of aesthetics we will use the alternative look  $\mathcal{O}_{ij} \equiv 1 : B_{ji}$ . These expressions then must be interpreted in the sense that an odds ratio equivalent to  $B_{ij} : 1$  means the model  $i$  is  $B_{ij}$  times more probable than model  $j$ , whereas and odds ratio of the form  $1 : B_{ji}$  means model  $i$  is  $B_{ji}$  times less probable than model  $j$ .

Before we close this section, an important remark is in order. The usual situation in cosmology is that for the task of constraining the parameters  $\{\theta_i\}$  one has at hand more than one set of statistically independent observational data, say  $\{d_j^{(1)}\}, \dots, \{d_k^{(m)}\}$ ; in that case, one can resort to the joint probability density function

$$p(\{\theta_i\}|\{d_j^{(1)}\} \cap \dots \cap \{d_k^{(m)}\}, \mathcal{M}) = p(\{\theta_i\}|\{d_j^{(1)}\}, \mathcal{M}) \times \dots \times p(\{\theta_i\}|\{d_k^{(m)}\}, \mathcal{M}). \quad (47)$$

Clearly, the latter rule can be used to generalize conveniently the whole discussion above to this situation with availability of more than one dataset.

## V. RESULTS AND CONCLUSIONS

---

In this paper we have performed parameter estimation and model selection for a set of flat FRW cosmological models which could be suitable to explain the observed current acceleration. Half of the models stem from the assumption of a dark energy component in the Universe,

---

whereas the other half is made by models motivated by extra dimensions and that include a gravitational component of the observed expansion acceleration. We analyze data coming from (most recent) SNIa luminosity, CMB shift and  $H(z)$  measurements. Even though most of our

TABLE II: Best fits,  $\chi^2$  and Credible Intervals

Model	Best-fit	$\chi^2/\text{dof}$	68% conf. int.	95% conf. int.
LCDM	$\Omega_m = 0.26$	1.03	$\Omega_m = 0.26_{-0.02}^{+0.02}$	$\Omega_m = 0.26_{-0.04}^{+0.05}$
DGP	$\Omega_m = 0.23$	1.08	$\Omega_m = 0.23_{-0.02}^{+0.02}$	$\Omega_m = 0.23_{-0.04}^{+0.04}$
QCDM	$\Omega_m = 0.24$ $w = -0.94$	1.03	$\Omega_m = 0.25_{-0.02}^{+0.03}$ $w = -0.96_{-0.09}^{+0.08}$	$\Omega_m = 0.25_{-0.05}^{+0.06}$ $w = -0.96_{-0.20}^{+0.15}$
LDGP	$\Omega_m = 0.26$ $\Omega_{r_c} = 0.00$	1.04	$\Omega_m = 0.26_{-0.02}^{+0.03}$ $\Omega_{r_c} = 0.00_{+0.02}$	$\Omega_m = 0.26_{-0.05}^{+0.05}$ $\Omega_{r_c} = 0.00_{+0.05}$
QDGP	$\Omega_m = 0.25$ $\Omega_{r_c} = 0.00$ $w = -0.95$	1.04	$\Omega_m = 0.23_{-0.03}^{+0.03}$ $\Omega_{r_c} = 0.00_{+0.88}$ $w = -0.81_{-0.07}^{+0.05}$	$\Omega_m = 0.23_{-0.05}^{+0.06}$ $\Omega_{r_c} = 0.00_{+2.32}$ $w = -0.81_{-0.19}^{+0.09}$
CPL	$\Omega_m = 0.25$ $w_0 = -1.08$ $w_1 = 0.58$	1.04	$\Omega_m = 0.26_{-0.03}^{+0.03}$ $w_0 = -1.05_{-0.20}^{+0.19}$ $w_1 = 0.37_{-0.84}^{+0.70}$	$\Omega_m = 0.26_{-0.05}^{+0.06}$ $w_0 = -1.05_{-0.47}^{+0.37}$ $w_1 = 0.37_{-1.78}^{+1.34}$

TABLE III: Priors

Model	Parameter ranges
LCDM	$0.00 \leq \Omega_m \leq 0.60$
DGP	$0.00 \leq \Omega_m \leq 0.60$
QCDM	$0.00 \leq \Omega_m \leq 0.60$ , $-1.50 \leq w \leq -0.33$
LDGP	$0.00 \leq \Omega_m \leq 0.60$ , $0.00 \leq \Omega_{r_c} \leq 0.10$
CPL	$0.00 \leq \Omega_m \leq 0.60$ , $-1.50 \leq w_0 \leq -0.33$ , $0.00 \leq w_1 \leq 2.00$
QDGP	$0.00 \leq \Omega_m \leq 0.60$ , $-1.50 \leq w \leq -0.33$ , $0.00 \leq \Omega_{r_c} \leq 1.00$

TABLE IV: Bayes evidence

Model	$\mathcal{E}$	$\ln(B_{i,\text{DGP}})$	$\ln(B_{i,\text{QCDM}})$	$\ln(B_{i,\text{LDGP}})$	$\ln(B_{i,\text{CPL}})$	$\ln(B_{i,\text{QDGP}})$
LCDM	$1.05 \times 10^{-46}$	5.55	1.54	2.31	1.83	3.56
DGP	$4.07 \times 10^{-49}$	0.00	-4.01	-3.24	-3.73	-2.00
QCDM	$2.25 \times 10^{-47}$		0.00	0.77	0.29	2.01
LDGP	$1.04 \times 10^{-47}$			0.00	-0.49	1.24
CPL	$1.69 \times 10^{-47}$				0.00	1.72
QDGP	$3.02 \times 10^{-48}$					0.00

statistical treatment fits into the Bayesian approach, for completeness we also report results on some frequentist estimators. Our results are consistent with partially overlapping work (e.g. [20, 21]) done previously using different combinations of observations.

One may think a priori the dominant source of error to be the  $H(z)$  data, as the percentage errors range from 8%

to 20%, whereas for the SN data the lowest percentage error is 0.3% and the highest is 1% on the one hand, and for the CMB shift single datum we have a percentage error of 1.7%. On the other hand, since the  $\chi^2$  construction from the  $H(z)$  data does not involve any integration, there might be a restraint in the propagation of errors coming from them. We are inclined to think this is actually the



TABLE V: Odds ratio (number of times a model is more probable than other)

Model	$\mathcal{O}_{i,DGP}$	$\mathcal{O}_{i,QCDM}$	$\mathcal{O}_{i,LDGP}$	$\mathcal{O}_{i,CPL}$	$\mathcal{O}_{i,QDGP}$
LCDM	258:1	5:1	10:1	6:1	35:1
DGP	1:1	1:55	1:26	1:42	1:7
QCDM		1:1	2:1	1:1	7:1
LDGP			1:1	1:2	3:1
CPL				1:1	6:1
QDGP					1:1

case as the size of errors in our study are comparable with those obtained in other works.

In the light of our results we conclude, first of all, that the frequentist estimator  $\chi^2/dof$  significantly disfavors the DGP model over all the other models considered. We compute the probability of getting values of the  $\chi^2$  not farther from the minimum than the minimum  $\chi^2$  for all other models, as defined in [25] and we get a probability  $P \geq 99\%$ . Consistently we arrive at the same conclusion using Bayes evidence. On the other hand, if we compare LCDM with all the other models, it turns out that from the frequentist perspective it is as good as QCDM, whereas for LDGP, CPL and QDGP one gets exactly the same value  $\chi^2/dof$ , a value which turns out to be just slightly larger than the one for LCDM. In conclusion, the frequentist analysis yields the result that LCDM is just marginally preferred over all the rest of the models, except for DGP which is clearly the least likely model of all six.

Regarding the Bayesian analysis, the reader can decide whether to qualify our results using the adjectives in Jeffrey’s scale or just stick to the objectivity of the numbers giving us the odds of the different models against the others, but at least in the case of DGP versus LCDM we dare

to say it is difficult not to be carried by the impression that it is rather disfavored.

Finally, our results on credible limits point us in the direction that this combination of data sets constrain very poorly models with two “dark energy” parameters, so parameter constraints on CPL and QDGP seem not to be tight enough.

### Acknowledgements

We are grateful to Roy Maartens for reading the manuscript, engaging in useful conversations and making encouraging comments. We acknowledge Luca Amendola for offering us his software from which part of our codes originates. Thanks to Mariam Bouhmadi-López, Rob Crittenden, Bob Nichol, Will Percival, Björn Schäfer, Roberto Trotta and Jussi Väliviita for enlightening discussions.

R.L. is supported by the University of the Basque Country through research grant GIU06/37 and by the Spanish Ministry of Education and Culture through the RyC program, and research grants FIS2004-01626 and FIS2004-0374-E.

---

## APPENDIX A: PROBABILITY DENSITIES

In this appendix we present the plots of the probability densities of the six different models considered. As explained above  $\mathcal{L}_{\theta_i}$  will represent the probability density obtained by marginalization over all the parameters of the model except for the parameter  $\theta_i$ . For the models with more than one parameter we also plot the likelihood contours associated to 68, 95 and 99% probability. For the models with 3 parameters we have fixed  $\Omega_m$  to be 0.25.

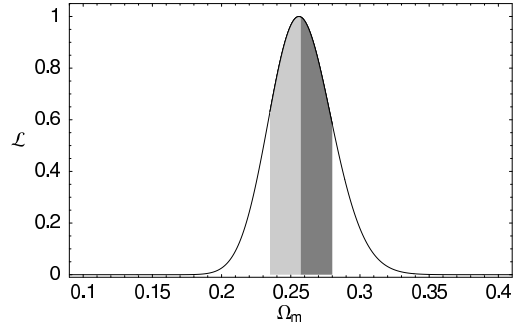


FIG. 1: Likelihood function for the flat LCDM model. The light (dark) shaded region indicates the error on  $\Omega_m$  to the left (right) of the median.

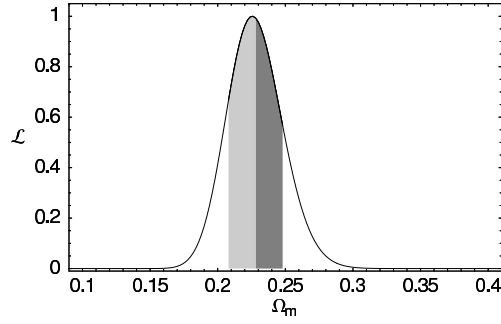


FIG. 2: Same as for fig.1 but for the flat DGP model.

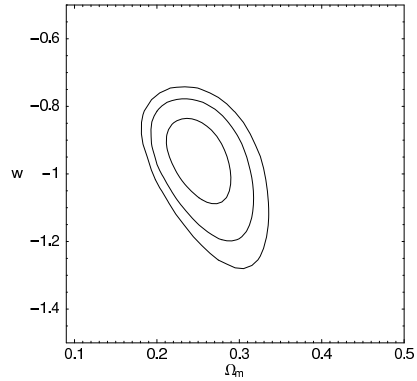


FIG. 3: Likelihood contours corresponding to the 68, 95 and 99% credible contours in the  $(w, \Omega_m)$  plane for the QCDM model.

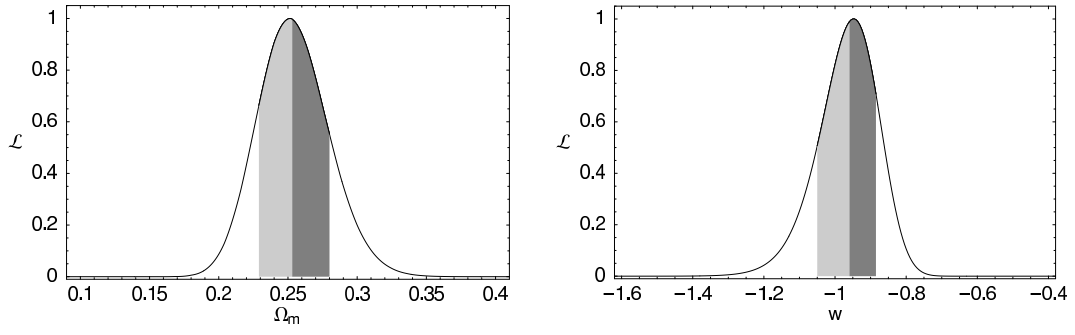


FIG. 4: Marginalized likelihood functions for the QCDM model for  $\Omega_m$  (left) and the equation of state  $w$  (right).

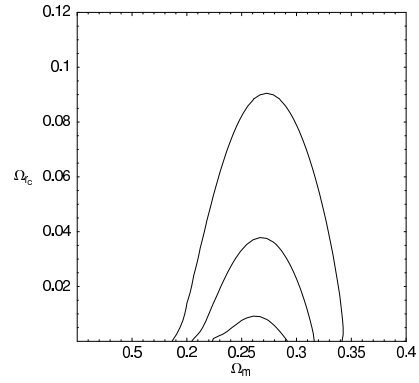


FIG. 5: Likelihood contours corresponding to the 68, 95 and 99% credible contours in the  $(\Omega_m, \Omega_{r_c})$  plane for the LDGP model.

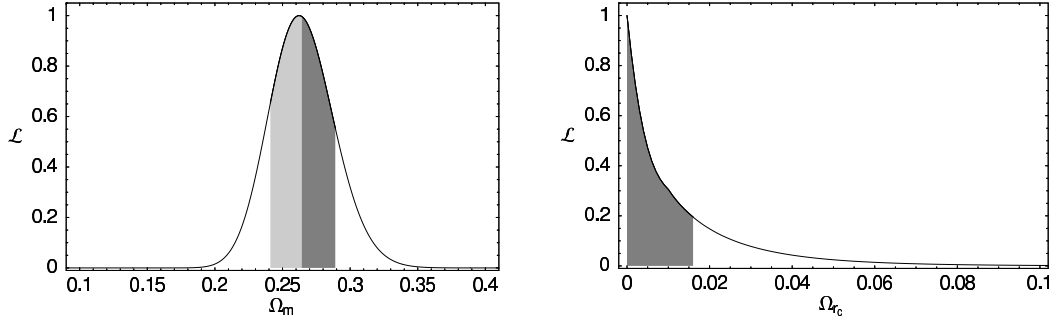


FIG. 6: Marginalized likelihood functions for the LDGP model for  $\Omega_m$  (left) and  $\Omega_r$  (right).

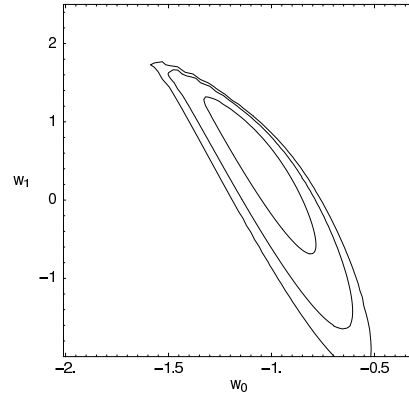


FIG. 7: Likelihood contours corresponding to the 68, 95 and 99% credible contours in the  $(w_0, w_1)$  plane for the CPL Ansatz.  $\Omega_m$  has been fixed to 0.25.

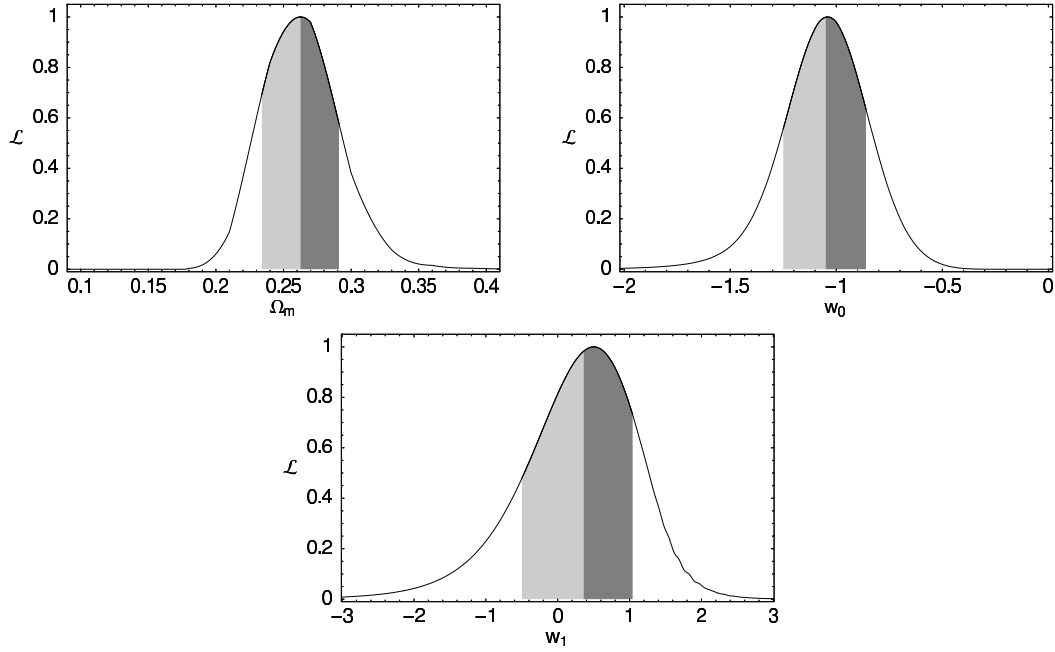


FIG. 8: Marginalized likelihood functions for the CPL model for  $\Omega_m$  (left top),  $w_0$  (right top) and  $w_1$  (bottom).

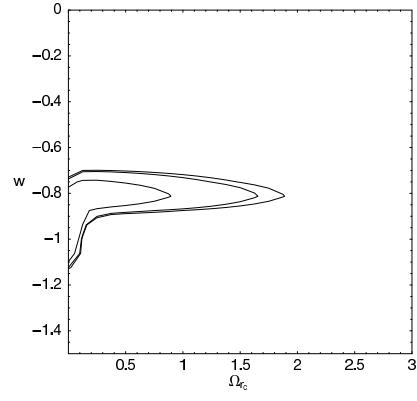


FIG. 9: Likelihood contours corresponding to the 68, 95 and 99% credible contours in the  $(\Omega_{r_c}, w)$  plane for the QDGP model.  $\Omega_m$  has been fixed to 0.25.

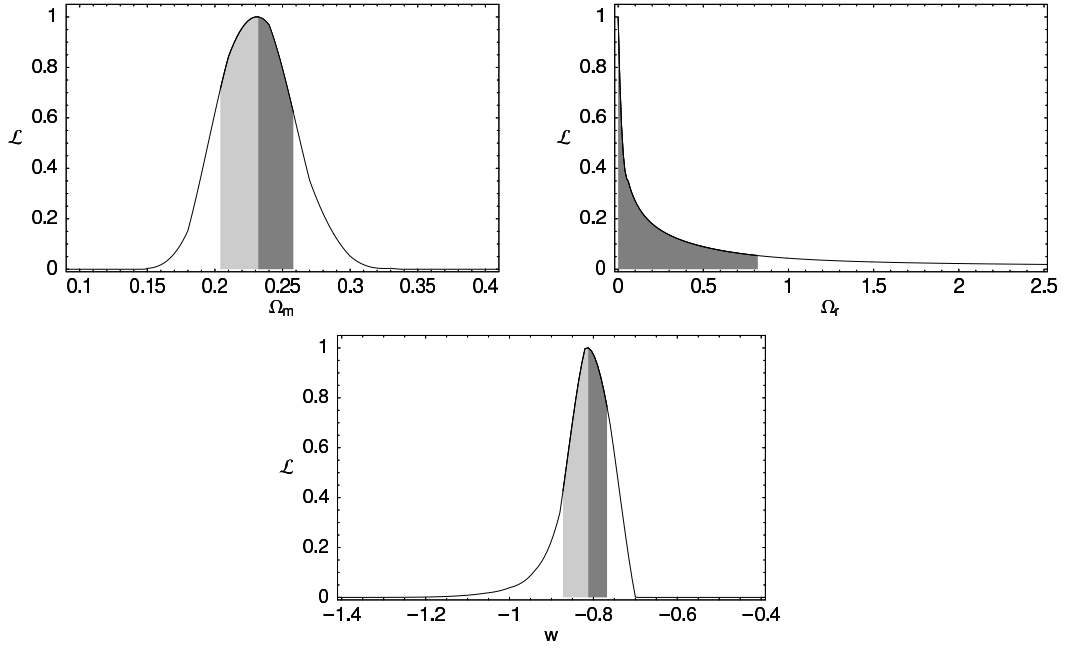


FIG. 10: Marginalized likelihood functions for the QDGP model for  $\Omega_m$  (left top),  $\Omega_r$  (right top) and  $w$  (bottom).

## APPENDIX B: EQUATION OF STATE PARAMETERS

For the sake of illustration, we represent the best fits  $w_{de}(z)$  for the CPL model and  $w_{\text{eff}}(z)$  for the DGP and LDGP models. We do not present the plots for the LCDM and QCDM models as the corresponding plots are basically stripes of constant width as they correspond to non-dynamical dark energy. For every best fit we include in the plot an estimation of error propagation based on the assumption of no error correlation. As in our parameter constraints, we have various sources of complication. On the one hand, as in some models (CPL, for instance) we have found slight departures from gaussianity, we cannot use the standard error propagation formula, in addition the errors found are large in the case of some parameters also we put forward a modification of the standard formula in order to account for non-gaussianities and large errors. Assuming our constraints in a generic cosmological parameter  $\theta_i$  are reported in the form  $\theta_{\text{imd}}^{+\Delta\theta_{iu}}_{-\Delta\theta_{il}}$ , with  $\Delta\theta_{il}$  and  $\Delta\theta_{iu}$  being positive quantities. We can give an estimate of the error in a quantity  $f(\theta_1, \dots, \theta_n)$  derived from various such parameters by taking for the upper error the quantity

$$\Delta f_u = \sqrt{\sum_{i=1}^n (\max(\Delta f_{iu}, -\Delta f_{il}))^2} \quad (\text{B1})$$

and for the lower error the quantity

$$\Delta f_l = \sqrt{\sum_{i=1}^n (\min(\Delta f_{iu}, -\Delta f_{il}))^2}, \quad (\text{B2})$$

where

$$\Delta f_{iu} = f(\dots \theta_{(i-1)\text{md}}, \theta_{\text{imd}} + \Delta\theta_{iu}, \theta_{(i+1)\text{md}}, \dots) - f(\dots \theta_{(i-1)\text{md}}, \theta_{\text{imd}}, \theta_{(i+1)\text{md}}, \dots) \quad (\text{B3})$$

and

$$\Delta f_{il} = f(\dots \theta_{(i-1)\text{md}}, \theta_{\text{imd}} - \Delta\theta_{il}, \theta_{(i+1)\text{md}}, \dots) - f(\dots \theta_{(i-1)\text{md}}, \theta_{\text{imd}}, \theta_{(i+1)\text{md}}, \dots). \quad (\text{B4})$$

So, we have proposed an estimation of error based on finite differences; nevertheless, one can be more refined if errors are small, i.e.  $\Delta\theta_{iu} = \delta\theta_{iu}$  and  $\Delta\theta_{il} = \delta\theta_{il}$ , because then one can write

$$\Delta f_u \simeq \delta f_u = \sqrt{\sum_{i=1}^n \left( \max \left( \frac{\partial f}{\partial \theta_i} \delta\theta_{iu}, -\frac{\partial f}{\partial \theta_i} \delta\theta_{il} \right) \right)^2}. \quad (\text{B5})$$

and

$$\Delta f_l \simeq \delta f_l = \sqrt{\sum_{i=1}^n \left( \min \left( \frac{\partial f}{\partial \theta_i} \delta\theta_{iu}, -\frac{\partial f}{\partial \theta_i} \delta\theta_{il} \right) \right)^2}. \quad (\text{B6})$$

Finally, in the gaussian situations ( $\Delta\theta_{iu} = \Delta\theta_{il} = \Delta\theta_i$ ) (as for instance DGP) we get  $\Delta f_u = \Delta f_l$ .

In Fig. (11) we depict the best fit equation of state parameter along with error stripes for the models with more than one parameter. A few points are worth mentioning regarding the LDGP and QDGP models so as to clarify the peculiarity of the result. First of all, one must keep in mind for both cases we have found the best fit to correspond to their LCDM limit, which translates into an exactly constant equation of state parameter. On the other hand, the LDGP may look even stranger, as no upper error stripe appears in its plot. The reason for this is well grounded analytically, as the LDGP model does not have the ability to cross the phantom divide [19], so  $w_{\text{eff}}$  cannot be error-propagated across that barrier. Our plot just gives a graphical account of that analytical impossibility.

[1] J. Simon, L. Verde and R. Jiménez, Phys. Rev. D **71** (2005) 123001 [arXiv:astro-ph/0412269].

[2] L. Samushia and B. Ratra, Astrophys. J. **650** (2006) L5

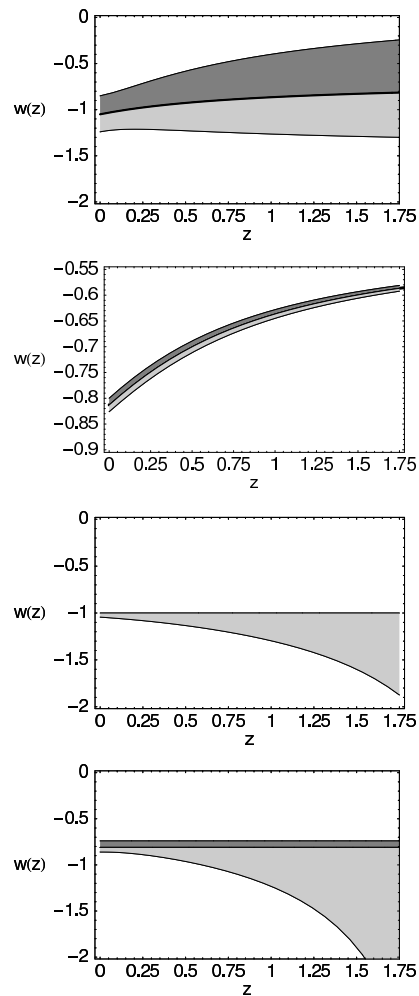


FIG. 11: Equation of state parameter as a function of redshift for models CPL, DGP, LDGP and QDGP (top to bottom). The black lines correspond to the best fit for each of them, and the gray bands indicate the errors (calculated by the finite differences method).

- [arXiv:astro-ph/0607301].
- [3] H. Wei and S. N. Zhang, Phys. Lett. B **644** (2007) 7 [arXiv:astro-ph/0609597]; P. Wu and H. W. Yu, Phys. Lett. B **644** (2007) 16 [arXiv:gr-qc/0612055]; P. X. Wu and H. W. Yu, JCAP **0703** (2007) 015 [arXiv:astro-ph/0701446]; L. I. Xu, C. W. Zhang, B. R. Chang and H. Y. Liu, arXiv:astro-ph/0701519; A. Kurek and M. Szydlowski, arXiv:astro-ph/0702484; H. Zhang and Z. H. Zhu, arXiv:astro-ph/0703245.
- [4] T. M. Davis *et al.*, arXiv:astro-ph/0701510.
- [5] Y. Wang and P. Mukherjee, Astrophys. J. **650** (2006) 1 [arXiv:astro-ph/0604051].
- [6] D. N. Spergel *et al.* [WMAP Collaboration], Astrophys. J. Suppl. **170** (2007) 377 [arXiv:astro-ph/0603449].
- [7] R. Maartens and E. Majerotto, Phys. Rev. D **74** (2006) 023004 [arXiv:astro-ph/0603353].
- [8] D. J. Eisenstein *et al.* [SDSS Collaboration], Astrophys. J. **633** (2005) 560 [arXiv:astro-ph/0501171].
- [9] A. G. Riess *et al.* [Supernova Search Team Collaboration], Astron. J. **116** (1998) 1009 [arXiv:astro-ph/9805201].
- [10] A. G. Riess *et al.* [Supernova Search Team Collaboration], Astrophys. J. **607** (2004) 665 [arXiv:astro-ph/0402512].
- [11] A. G. Riess *et al.*, Astrophys. J. **659** (2007) 98 [arXiv:astro-ph/0611572].
- [12] For reviews see e.g. S. Tsujikawa, arXiv:hep-ph/0304257, N. Turok, Class. Quant. Grav. **19** (2002) 3449.
- [13] C. L. Bennett *et al.* [WMAP Collaboration], Astrophys. J. Suppl. **148** (2003) 1 [arXiv:astro-ph/0302207]; D. N. Spergel *et al.* [WMAP Collaboration], Astrophys. J. Suppl. **148** (2003) 175 [arXiv:astro-ph/0302209].
- [14] G. R. Dvali, G. Gabadadze and M. Porrati, Phys. Lett. B **485** (2000) 208 [arXiv:hep-th/0005016].
- [15] C. Deffayet, Phys. Lett. B **502** (2001) 199 [arXiv:hep-th/0010186].
- [16] V. Sahni and Y. Shtanov, JCAP **0311** (2003) 014 [arXiv:astro-ph/0202346]; A. Lue and G. D. Starkman, Phys. Rev. D **70** (2004) 101501 [arXiv:astro-ph/0408246].

- [17] M. Chevallier and D. Polarski, *Int. J. Mod. Phys. D* **10** (2001) 213 [arXiv:gr-qc/0009008].
- [18] E. V. Linder, *Phys. Rev. Lett.* **90** (2003) 091301 [arXiv:astro-ph/0208512].
- [19] L. P. Chimento, R. Lazkoz, R. Maartens and I. Quiros, *JCAP* **0609** (2006) 004 [arXiv:astro-ph/0605450].
- [20] P. Serra, A. Heavens and A. Melchiorri, arXiv:astro-ph/0701338, V. Barger, Y. Gao and D. Marfatia, *Phys. Lett. B* **648** (2007) 127 [arXiv:astro-ph/0611775], E. L. Wright, arXiv:astro-ph/0701584.
- [21] S. Rydbeck, M. Fairbairn and A. Goobar, arXiv:astro-ph/0701495.
- [22] G. B. Zhao, J. Q. Xia, H. Li, C. Tao, J. M. Virey, Z. H. Zhu and X. Zhang, *Phys. Lett. B* **648** (2007) 8 [arXiv:astro-ph/0612728]; N. Pires, Z. H. Zhu and J. S. Alcañiz, *Phys. Rev. D* **73** (2006) 123530 [arXiv:astro-ph/0606689]; C. Zunckel and R. Trotta, arXiv:astro-ph/0702695; Y. Gong, A. Wang, Q. Wu and Y. Z. Zhang, arXiv:astro-ph/0703583.
- [23] V. Sahni and A. Starobinsky, V. Sahni and A. Starobinsky, *Int. J. Mod. Phys. D* **15** (2006) 2105 [arXiv:astro-ph/0610026].
- [24] A. A. Starobinsky, *JETP Lett.* **68** (1998) 757 [Pisma Zh. Eksp. Teor. Fiz. **68** (1998) 721 [arXiv:astro-ph/9810431]; D. Huterer and M. S. Turner, *Phys. Rev. D* **60** (1999) 081301 [arXiv:astro-ph/9808133]; T. D. Saini, S. Raychaudhury, V. Sahni and A. A. Starobinsky, *Phys. Rev. Lett.* **85** (2000) 1162 [arXiv:astro-ph/9910231]; T. Chiba and T. Nakamura, *Phys. Rev. D* **62** (2000) 121301 [arXiv:astro-ph/0008175]; D. A. Dicus and W. W. Repko, arXiv:astro-ph/0605537.
- [25] R. Lazkoz, S. Nesseris and L. Perivolaropoulos, *JCAP* **0511** (2005) 010 [arXiv:astro-ph/0503230].
- [26] J. Weller and A. Albrecht, *Phys. Rev. D* **65** (2002) 103512 [arXiv:astro-ph/0106079]; B. F. Gerke and G. Efstathiou, *Mon. Not. Roy. Astron. Soc.* **335** (2002) 33 [arXiv:astro-ph/0201336]; I. Maor, R. Brustein, J. McMahon and P. J. Steinhardt, *Phys. Rev. D* **65** (2002) 123003 [arXiv:astro-ph/0112526]; P. S. Corasaniti and E. J. Copeland, *Phys. Rev. D* **67** (2003) 063521 [arXiv:astro-ph/0205544]; E. V. Linder, *Phys. Rev. Lett.* **90** (2003) 091301 [arXiv:astro-ph/0208512]; Y. Wang and P. Mukherjee, *Astrophys. J.* **606** (2004) 654 [arXiv:astro-ph/0312192]; T. D. Saini, J. Weller and S. L. Bridle, *Mon. Not. Roy. Astron. Soc.* **348** (2004) 603 [arXiv:astro-ph/0305526]; S. Nesseris and L. Perivolaropoulos, *Phys. Rev. D* **70** (2004) 043531 [arXiv:astro-ph/0401556]; S. Nesseris and L. Perivolaropoulos, *Phys. Rev. D* **72** (2005) 123519 [arXiv:astro-ph/0511040]; Y. G. Gong, *Int. J. Mod. Phys. D* **14** (2005) 599 [arXiv:astro-ph/0401207]; Y. G. Gong, *Class. Quant. Grav.* **22** (2005) 2121 [arXiv:astro-ph/0405446]; H. K. Jassal, J. S. Bagla and T. Padmanabhan, *Mon. Not. Roy. Astron. Soc.* **356** (2005) L11 [arXiv:astro-ph/0404378]; B. Feng, M. Li, Y. S. Piao and X. Zhang, *Phys. Lett. B* **634** (2006) 101 [arXiv:astro-ph/0407432]; J. P. Uzan, *Gen. Rel. Grav.* **39** (2007) 307 [arXiv:astro-ph/0605313].
- [27] S. Nesseris and L. Perivolaropoulos, *Phys. Rev. D* **72** (2005) 123519 [arXiv:astro-ph/0511040].
- [28] V. Sahni, T. D. Saini, A. A. Starobinsky and U. Alam, *JETP Lett.* **77** (2003) 201 [Pisma Zh. Eksp. Teor. Fiz. **77**, 249 (2003)] [arXiv:astro-ph/0201498]; U. Alam, V. Sahni, T. D. Saini and A. A. Starobinsky, *Mon. Not. Roy. Astron. Soc.* **344** (2003) 1057 [arXiv:astro-ph/0303009]. U. Alam, V. Sahni, T. D. Saini and A. A. Starobinsky, *Mon. Not. Roy. Astron. Soc.* **354** (2004) 275 [arXiv:astro-ph/0311364]; U. Alam, V. Sahni and A. A. Starobinsky, *JCAP* **0406** (2004) 008 [arXiv:astro-ph/0403687].
- [29] R. Lazkoz, R. Maartens and E. Majerotto, *Phys. Rev. D* **74** (2006) 083510 [arXiv:astro-ph/0605701].
- [30] R. Jimenez and A. Loeb, *Astrophys. J.* **573** (2002) 37 [arXiv:astro-ph/0106145].
- [31] R. Jimenez, L. Verde, T. Treu and D. Stern, *Astrophys. J.* **593** (2003) 622 [arXiv:astro-ph/0302560].
- [32] R. G. Abraham *et al.*, *Astron. J.* **127** (2004) 2455 [arXiv:astro-ph/0402436].
- [33] J. Dunlop, J. Peacock, H. Spinrad, A. Dey, R. Jimenez, D. Stern and R. Windhorst, *Nature* **381** (1996) 581; H. Spinrad, A. Dey, D. Stern, J. Dunlop, J. Peacock, R. Jimenez and R. Windhorst, *Astrophys. J.* **484** (1997) 581 [arXiv:astro-ph/9702233]; T. Treu, M. Stiavelli, S. Casertano, P. Moller, and G. Bertin, *Mon. Not. Roy. Astron. Soc.* **308** (1999) 1037 [arXiv:astro-ph/9904327]; T. Treu, M. Stiavelli, P. Moller, S. Casertano and G. Bertin, *Mon. Not. Roy. Astron. Soc.* **326** (2001) 221 [arXiv:astro-ph/0104177]; T. Treu, M. Stiavelli, S. Casertano, P. Moller, and G. Bertin, *Astrophys. J. Lett.* **564** (2002) L13 [arXiv:astro-ph/0111504]; L. A. Nolan, J. S. Dunlop, R. Jiménez and A. F. Heavens, *Mon. Not. Roy. Astron. Soc.* **341**, 464 (2003) [arXiv:astro-ph/0103450].
- [34] R. Jimenez, J. MacDonald, J. S. Dunlop, P. Padoan and J. A. Peacock, *Mon. Not. Roy. Astron. Soc.* **349** (2004) 240 [arXiv:astro-ph/0402271].
- [35] S. L. Bridle, R. Crittenden, A. Melchiorri, M. P. Hobson, R. Kneissl and A. N. Lasenby, *Mon. Not. Roy. Astron. Soc.* **335** (2002) 1193 [arXiv:astro-ph/0112114].
- [36] M. Bonamente, M. K. Joy, S. J. La Roque, J. E. Carlstrom, E. D. Reese and K. S. Dawson, *Astrophys. J.* **647** (2006) 25 [arXiv:astro-ph/0512349].
- [37] W. L. Freedman *et al.*, *Astrophys. J.* **553** (2001) 47 [arXiv:astro-ph/0012376].
- [38] W. M. Wood-Vasey *et al.*, arXiv:astro-ph/0701041.
- [39] P. Astier *et al.*, *Astron. Astrophys.* **447** (2006) 31 [arXiv:astro-ph/0510447].
- [40] M. Hamuy, M. M. Phillips, N. B. Suntzeff, R. A. Schommer and J. Maza, *Astron. Jour.* **112** (1996) 2408 [arXiv:astro-ph/9609064].
- [41] S. Jha, A. G. Riess and R. P. Kirshner, *Astrophys. J.* **659** (2007) 122 [arXiv:astro-ph/0612666].
- [42] A. Goobar, 2006 private communication.
- [43] E. Di Pietro and J. F. Claeskens, *Mon. Not. Roy. Astron. Soc.* **341** (2003) 1299 [arXiv:astro-ph/0207332]; S. Nesseris and L. Perivolaropoulos, *Phys. Rev. D* **70** (2004) 043531 [arXiv:astro-ph/0401556]; O. Elgaroy and T. Multamäki, *JCAP* **0609** (2006) 002 [arXiv:astro-ph/0603053].
- [44] J. R. Bond, G. Efstathiou and M. Tegmark, *Mon. Not. Roy. Astron. Soc.* **291** (1997) L33 [arXiv:astro-ph/9702100].
- [45] W. J. Percival *et al.* [The 2dFGRS Team Collaboration], *Mon. Not. Roy. Astron. Soc.* **337** (2002) 1068 [arXiv:astro-ph/0206256].
- [46] S. Nesseris and L. Perivolaropoulos, *JCAP* **0701** (2007) 018 [arXiv:astro-ph/0610092].



- [47] O. Elgaroy and T. Multamäki, arXiv:astro-ph/0702343.
- [48] E. L. Wright, arXiv:astro-ph/0701584.
- [49] Y. Wang and P. Mukherjee, arXiv:astro-ph/0703780.
- [50] J. Väliiviita, PhD thesis, Helsinki Institute of Physics (2005).
- [51] R. Trotta, PhD thesis, University of Geneva (2004).
- [52] R. Trotta, Mon. Not. R. Astron. Soc., **378** (2007) 72.
- [53] R. Trotta, 2007 private communication.
- [54] R.D. Cousins, Am. J. Phys. **63** (1995) 5.
- [55] G. Zech, arXiv:hep-ex/0004011.
- [56] J. Väliiviita, 2006 private communication.
- [57] D.G. T. Denison, C.C. Holmes, B.K. Mallick, A.F.M. Smith, *Bayesian Methods for Nonlinear Classification and Regression (Wiley Series in Probability and Statistics)*, (John Wiley & Sons, 2004).
- [58] A. R. Liddle, P. Mukherjee and D. Parkinson, Astron. Geophys. **47** (2006) 4.30. [arXiv:astro-ph/0608184].
- [59] H. Jeffreys, *The Theory of Probability (Oxford Classic Texts in the Physical Sciences)* (Oxford University Press, 3rd. ed., 1998)
- [60] L. Wasserman, Carnegie Mellon University Statistics Department Technical Report No. 666, 1997.